

Accepted Manuscript

Effect of displacement damage level on the ion-irradiation affected zone evolution in W single crystals

Eva Hasenhuettl, Zhexian Zhang, Kiyohiro Yabuuchi, Akihiko Kimura



PII: S0022-3115(17)30332-X

DOI: [10.1016/j.jnucmat.2017.08.030](https://doi.org/10.1016/j.jnucmat.2017.08.030)

Reference: NUMA 50471

To appear in: *Journal of Nuclear Materials*

Received Date: 6 March 2017

Revised Date: 6 July 2017

Accepted Date: 21 August 2017

Please cite this article as: E. Hasenhuettl, Z. Zhang, K. Yabuuchi, A. Kimura, Effect of displacement damage level on the ion-irradiation affected zone evolution in W single crystals, *Journal of Nuclear Materials* (2017), doi: 10.1016/j.jnucmat.2017.08.030.

This is a PDF file of an unedited manuscript that has been accepted for publication. As a service to our customers we are providing this early version of the manuscript. The manuscript will undergo copyediting, typesetting, and review of the resulting proof before it is published in its final form. Please note that during the production process errors may be discovered which could affect the content, and all legal disclaimers that apply to the journal pertain.

1 **Effect of displacement damage level on the ion-irradiation affected zone evolution in W**
 2 **single crystals**

3

4 Eva Hasenhuettl^{*1}, Zhexian Zhang², Kiyohiro Yabuuchi², Akihiko Kimura²

5 ¹ Graduate School of Energy Science, Kyoto University, Yoshida-honmachi, Sakyo-ku, Kyoto
 6 606-8501, Japan

7 ² Institute of Advanced Energy (IAE), Kyoto University, Gokasho, Uji, Kyoto 611-0011, Japan

8 *Corresponding author: Eva Hasenhuettl, eva-hasenhuettl@iae.kyoto-u.ac.jp

9

10 **Abstract:**

11 Pure tungsten (W) single crystals of (001) and (011) surface orientations, denoted as
 12 W{001} and W{011}, respectively, were irradiated with 6.4 MeV Fe³⁺ ions up to the
 13 displacement damages of 0.1 and 2 dpa at 573 K. Nanoindentation (NI) hardness measurements
 14 showed that the hardness profiles of both the W single crystals were independent of the damage
 15 level and kept the same trend of the orientation dependence that the hardening profile of NI
 16 hardness was deeper in W{001} than W{011}. In contrast, TEM examinations revealed that the
 17 ion-irradiation affected zone evolution was remarkably influenced by the damage level showing
 18 1.5 times deeper extended ion-irradiation affected zone in W{001} than in W{011} after
 19 irradiation to 2 dpa, while no such an orientation dependence was observed after irradiation to
 20 0.1 dpa. In W{011}, the ion-irradiation affected zone sizes almost matched the target depth
 21 results of SRIM code calculation irrespective of damage level. At the displacement damage of 1
 22 and 2 dpa, a double black band structure with a number of ordered networks of dislocation loop
 23 rafts was observed in both the W{001} and W{011}, while in the case of 0.1dpa, the major
 24 defect type in W{001} was isolated dislocation loops and those in W{011} was dislocation loop
 25 rafts. The TEM microstructural evolution affected by damage level and crystal orientation was
 26 interpreted in terms of 1D motion of dislocation loops.

27 Keywords: tungsten single crystals; ion-irradiation hardening; damage level; orientation
 28 dependence; double black band; defect migration

1 **1. Introduction**

2 Tungsten (W) is considered to be the plasma facing material in ITER and DEMO fusion
 3 reactors where understanding radiation effects on W has been required for a safe divertor
 4 operation. Ion-irradiation experiment is often effective to investigate radiation effects on
 5 materials without time consumption, and in most of the previous studies, polycrystalline W was
 6 used to investigate the irradiation effects on W neglecting orientation dependence [1-5], while a
 7 few studies [6-13] suggested that ion-irradiation effects on W depended on crystal orientation.

8 Grzonka et al. [12] proposed that the ion-irradiation affected zone could depend on the
 9 orientation of the irradiated grain with respect to the ion beam direction. Their TEM observations
 10 showed small changes in the ion-irradiation affected zone, where the zone depth in a $<110>$
 11 grain was slightly deeper compared to that of the adjacent $<012>$ grain after self-ion irradiation
 12 to 2.3 dpa at room temperature. In addition, the zone size at 6.4 dpa showed a slight increase
 13 compared to the case at 2.3 dpa, but no grain dependent analysis was given further in their study.
 14 They considered that channeling and/or the interaction of dislocation with grain boundaries in
 15 the damage zone could be the reason for the difference in the detected damage depth, but no
 16 clear experimental evidence was reported.

17 Previously we discussed the ion-irradiation effects on hardening and microstructure of W
 18 single crystals after irradiation at 573K to 1 dpa [13], where the TEM examination revealed that
 19 there is no significant orientation dependence in the radiation damaged structure, while the depth
 20 profile of ion-irradiation hardening evaluated by nanoindentation (NI) turned out to be clearly
 21 orientation dependent. No conclusive mechanism, however, was provided in the previous study
 22 and a systematic study on the crystal orientation dependence and damage level dependence of
 23 irradiation effects in single crystal W is necessary.

24 As for the methodology of NI hardness measurement, the concepts of Nix and Gao [14],
 25 describing a hardness, H_0 , at infinite depth, $h=\infty$, were applied to the evaluation of ion-
 26 irradiation hardening by defining the so called “bulk equivalent” hardness by Kasada et al. [15].
 27 Since the NI hardness is influenced by many experimental conditions including heterogeneity of
 28 microstructures, the NI hardness measurements with single crystals may provide insights into the
 29 effect of grain boundaries on the NI hardness.

1 In this study, the effect of displacement damage level on the ion-irradiation affected zone
 2 evolution in W single crystals is investigated to understand the crystal orientation effect on the
 3 ion-irradiation hardening and microstructural evolution in W. Furthermore, NI hardness
 4 measurement is carried out to discuss “bulk equivalent” hardness [15] as a function of damage
 5 level and crystal orientation.

6

7 **2. Experimental Method**

8 The material used in his study was a W single crystal of 99.7% purity. From the W single
 9 crystal, small specimen with the surface orientations of (001) and (011) were cut and hereby
 10 denoted as W{001} and W{011}, respectively. The exact surface orientation of the specimens
 11 was measured by electron backscatter diffraction patterns. The detailed specimen preparation
 12 procedure was described in our previous study [13].

13 All the specimens were irradiated using a tandemron accelerator, DuET, at Kyoto
 14 University with 6.4 MeV Fe³⁺ ions up to a nominal damage level of 0.1 and 2 dpa at 573 K. The
 15 ion-beam was scanning with frequency 1000 Hz to X direction and 300 Hz to Y direction. In
 16 each case, the beam direction was set perpendicular to the surface of the respective W specimen.
 17 The specimens were heated with Joule heating and controlled by the electric current measuring
 18 with a pyrometer. The pressures were at the level of 10⁻⁷ Pa at 573K. At the end of the irradiation,
 19 the electric current was shut down and the specimen was cooled down to room temperature in the
 20 vacuum chamber.

21 The depth profile of the ion-irradiation induced displacement damage is calculated by
 22 SRIM code [16] using “Quick calculation of Damage” mode with the Kinchin and Pease model
 23 following the “energy damage” method introduced by Stoller et al. [17]. The damage- and iron
 24 distributions for the various damage levels including the irradiation condition of previous study
 25 [13] are given in Fig. 1. The nominal dpa is defined as the displacement damage occurring at the
 26 depth of 600 nm and the threshold energy is set to 90 eV [18]. As shown in Fig. 1, the ion-
 27 irradiation induced damaged zone reaches up to 1800 nm target depth, h_{target} , which is
 28 independent of the damage level.

1 For TEM microstructural examinations, thin foils were sampled by a focused ion beam
 2 (FIB) system (HITACHI FB2200) and the damage caused by FIB process was removed by
 3 subsequent flash electrolytic polishing (4-6 ms in 0.45% NaOH aqueous solution at 20 V at 276-
 4 277 K). TEM microstructure observation was performed with JEOL JEM-2010 at 200 kV.

5 The hardness of the specimens before and after ion-irradiation was measured by a
 6 nanoindenter (Agilent Technologies Inc. Model NanoIndenter G200) using a Berkovich tip. The
 7 area function of the tip has been calibrated using Oliver and Pharr method [19]. One basis of the
 8 Berkovich triangle tip was positioned perpendicular to a <111> sample orientation to maintain
 9 same azimuthal orientation of the tip in all the tested W specimens. For details on the positioning
 10 of the tip, see the reference [20]. Constant strain rate (CSR) test method including continuous
 11 stiffness method (CSM) [21] was performed. The testing conditions were as follows: the
 12 maximum contact depth was 2000 nm, the nominal strain rate was 0.05 s^{-1} , the oscillation
 13 amplitude was 1 nm and the testing temperature was $(299 \pm 2) \text{ K}$. For each testing condition, 10
 14 tests were carried out and the tests results beyond an uncertainty of $\pm 0.2 \text{ GPa}$ are neglected.

15 The “bulk” equivalent hardness of the ion-irradiated W was obtained by the least square
 16 fitting of the hardness data up to a hardness “shoulder” position, h_{crit} , that is the transition point
 17 where the unirradiated substrate starts to plastically deform [15]. The hardness “shoulder”
 18 position is originally denoted as a critical indentation depth in film, namely, the thickness of film,
 19 on substrate systems [22]. It was assumed that the NI hardness of thin film is not remarkably
 20 influenced by the underlying substrate when the indentation depth is smaller than h_{crit} [22]. Also
 21 a few reports coped with the correlation between plastic zone sizes below indentations and ion-
 22 irradiation affected zone sizes [23-25].

23

24 3. Results

25 3.1. NI-hardness Profiles

26 Fig. 2 a), c) and e) show the NI hardness, H , and indentation depth, h , ($H-h$) profile and
 27 Fig. 2 b), d) and f) show the H^2-l/h profile of unirradiated and irradiated W single crystals (0.1
 28 dpa: a) and b)), 1 dpa: c) and d)) [13] and 2 dpa: e) and f)). The H^2-l/h profile is according to the
 29 depth dependence of hardness after Nix and Gao interpretation [14] as mentioned before. It is

1 evident that there is at least one hardness “shoulder” position visible in the $H\text{-}h$ profiles and $H^2\text{-}$
 2 $I\text{/}h$ profiles of all the irradiated samples.

3 As for the orientation dependence, we previously showed that h_{crit} is deeper in 1 dpa W{001}
 4 compared to W{011} irradiated to 1 dpa [13]. In the present study, h_{crit} is slightly pronounced by
 5 increasing the damage level from 0.1 dpa to 2 dpa and it shows a definite orientation dependence
 6 in all damage levels.

7 The shape of the $H\text{-}h$ profile of W{011} irradiated to 2 dpa is similar to that observed in
 8 polycrystalline W irradiated to 2 dpa at the same temperature of 573 K as reported by Zhang et al.
 9 [1]. In contrast, in the case of W{001} irradiated to 2 dpa, a much deeper hardening profile
 10 compared to all other $H\text{-}h$ profiles was found with reflecting much deeper ion-irradiation
 11 affected zone (see later in session 3.2.2). In the unirradiated condition, W{001} shows higher
 12 hardness values up to 800 nm indentation depth than W{011}, while 800 nm both $H\text{-}h$ profiles
 13 follow the same trend.

14

15 3.2. Microstructural Examinations

16 3.2.1. Lower Displacement Damage (0.1 dpa)

17 The microstructural overviews of W{001} and W{011} irradiated to 0.1 dpa, denoted as
 18 0.1 dpa W{001} and 0.1 dpa W{011}, respectively herein after, are shown in Fig. 3. The
 19 irradiation induced damaged zone depth observed by TEM is about 1800 nm in 0.1 dpa W{011}
 20 and about 1900 nm in 0.1 dpa W{001} which matches well with SRIM code predictions in Fig. 1.
 21 The damage zone depth can thus be recognized as independent of crystal orientation in this
 22 irradiation condition. The major defect types in both orientations are dislocation loops; as shown
 23 in Fig. 4, the dislocation loops in 0.1 dpa W{011} were mostly merged to loop rafts in the entire
 24 ion-irradiation affected zone, whereas in 0.1 dpa W{001} most of the loops were isolated and
 25 interacting with line dislocations. In both orientations, a black band was observed at the end of
 26 the ion-irradiation affected zone with a width of around 400 nm for 0.1 dpa W{011} and around
 27 500 nm for 0.1 dpa W{001}.

1 Using a polycrystalline W, Yi et al. [6,7] reported that the formation of ion-irradiation
 2 induced loop strings and loop rafts required a higher irradiation temperature or damage level in
 3 <001> W than in non <001> W grains. Yi et al. [6,7] attributed the grain orientation dependence
 4 to the preferential loss of loop variants to the irradiation surface, where the probability of loop
 5 loss through glide in <001> grains is equal for all variants of $\frac{1}{2} <111>$ loops. Thus, the formation
 6 of loop string at the nearby free surface seems to favour in non <001> grains and lower the
 7 critical irradiation temperature and irradiation dose level [6,7]. However, in this study, the case
 8 of the 0.1 dpa W{001} specimen in the present study, we also found a high density of line
 9 dislocations in the irradiated zone by irradiation even at 573 K (see Fig. 4 a)-b)). On the other
 10 hand, smaller densities of line dislocations were observed in the 0.1 dpa W{011} specimen. We
 11 basically agree with the Yi et al.'s [6,7] proposed mechanism in the view point of the presence of
 12 four variants of $\frac{1}{2} <111>$ loops that can move to the free surface. Since we observed higher
 13 density of dislocations in W{001}, however, the loss of dislocation loops at the free surface
 14 would not so happen that the dislocation density is higher in W{001}. Namely, the large number
 15 of $\frac{1}{2} <111>$ loops variants provides more dislocation loops for accumulation near the free
 16 surface.

17

18 **3.2.2. Higher Displacement Damage (2 dpa)**

19 In the previous TEM observation on 1 dpa W{001} and 1 dpa W{011} irradiated at 573
 20 K [13], the microstructural overview showed a double black band structure consisting mainly of
 21 dislocation loop rafts and almost no orientation dependence was recognized in the
 22 microstructural evolution at 1 dpa.

23 However, in the present study, significantly different orientation dependence was found
 24 at 2 dpa, as presented in Fig. 6. The ion-irradiation affected damaged zone in 2 dpa W{001} is
 25 remarkably extended to a deeper region than that in 2 dpa W{011} indicating strong orientation
 26 dependence. The damaged zone in 2 dpa W{001} is spreading to 3100 nm depth, which is far
 27 beyond the SRIM code calculation results given in Fig. 1. On the other hand, the zone size in 2
 28 dpa W{011} is similar to the SRIM results indicating that the damaged zone is spreading to only
 29 1900 nm, which is similar to polycrystalline W irradiated to 2 dpa at the same temperature 573 K
 30 [1], where the deeper ion-irradiation affected zone reaches up to around 2000 nm [1].

1 As shown in Fig. 5, a double black band structure was also observed in both W single
 2 crystals after 2 dpa irradiation, where the black bands mainly consisted of dislocation loop rafts
 3 irrespective of the crystal orientation. Detailed microstructural examinations of the deeper high
 4 defect density band revealed that in both W single crystals, an ordered network of loop rafts
 5 along $\langle 111 \rangle$ is formed, see Fig. 6, and its upper and lower boundary is clearly distinguishable
 6 from the lower defect density region.

7

8 **4. Discussions**

9 **4.1. Bulk Equivalent Hardness**

10 By the H^2 - $1/h$ plots, the characteristic hardness “shoulders” arising at h_{crit} [15] are clearly
 11 observable. h_{crit} is larger in W{001} than in W{011} for each damage level and h_{crit} increases in
 12 both orientations with increasing damage level. Interestingly, 1 dpa and 2 dpa W{001} show an
 13 additional hardness shoulder at deeper indentation depth. This could be attributed to the two
 14 black bands in these irradiation conditions. However, this is not found in the 1 dpa and 2 dpa
 15 W{011}, probably because the shallower hardness shoulder appears in such small indentation
 16 depth that two shoulder points are not distinguishable in the H - h profiles. Also the NI-hardness
 17 before the hardness shoulder in 1 dpa W{001} is higher than in 2dpa W{001}, indicating a
 18 higher irradiation defect density in shallow depth in the 1 dpa condition, which confirms the
 19 trend that the defect formation tendency is observable to deeper bulk material with increasing
 20 damage level. h_{crit} values together with the irradiation hardening and bulk equivalent hardness
 21 values are summarized in Table 1 for one indentation test only that is considered to be
 22 representative due to the small error bar.

23 Fig. 7 shows that the irradiation hardening is already high at 0.1 dpa, indicating that the
 24 irradiation hardening differs between the two different orientations. Saturation of hardening
 25 seems to occur already at 1 dpa.

26

27

28 **4.2. Microstructural Examinations**

1 **4.2.1. Orientation Dependence of High Defect Density Zones**

2 In the previous study [13], it was considered that the 1D motion of very fine interstitial
 3 loops are not detectable by TEM but responsible for the irradiation hardening and the difference
 4 in the geometrical orientation of the direction of the 1D motion along the direction parallel to the
 5 Burger's vector, \mathbf{b} , of the loops causes the longer distance of the 1D motion of interstitial loops
 6 in W{001} than in W{011} [13]. Also here at 2 dpa, the large difference in ion-irradiation
 7 affected zone in 2 dpa W{001} compared to 2 dpa W{011} is also interpreted in terms of 1D
 8 motion of dislocation loops. It is considered that at high damage level, like 2 dpa, the interstitial
 9 loops can grow to the minimum size required to be visible by TEM but still exhibiting high
 10 mobility. TEM images are now indicating a remarkable difference in the range of the irradiation
 11 affected zone between the two orientations as shown in Fig. 5.

12 As for the characteristic feature of loop rafts as shown in Fig. 6, TEM examinations
 13 revealed that the loop rafts lay along <111> which was not accordance to the beam directions,
 14 <001> and <011> in Fig. 6(a) and (b), respectively. Because of the high dose of ion-irradiation,
 15 the dislocation loops grow to the visible size by TEM and move to the <111> directions.
 16 Consequently, the loop rafts were formed along <111>.

17

18

19 **4.2.2. Damage Level Dependence of High Defect Density Zones**

20 Fig. 8 a)-f) shows the ion-irradiation affected zone sizes of W{001} and W{011}
 21 observed in the present study together with those in our previous study [13]; the ion-irradiation
 22 affected zone size depends on damage level and crystal orientation. As for the formation
 23 mechanism of the double band, it can be interpreted in terms of the mutual annihilation of mobile
 24 interstitial dislocation loops and less mobile vacancy and their clusters. The distribution range of
 25 mobile interstitial dislocation loops may expand more than the damage profile obtained by SRIM
 26 code calculation but that of less mobile vacancy may be limited to the position shown by SRIM
 27 code calculation. In the region where the amount of interstitial atoms and vacancies is
 28 comparable, radiation defects may not be formed because of the mutual annihilation which may

1 form defect free zone in the depth range deeper than 1.2 μm with a wider distance because of
 2 expanded distribution of mobile interstitial dislocation loops.

3 Channelling effects could be considered for the effects of crystal orientation on the NI
 4 hardness profile and microstructural evolution in ion-irradiated W. As suggested in the
 5 introduction, most of previous research indicated that there was no remarkable channelling effect
 6 in W. The loop raft formation along some direction could be the evidence of channelling.
 7 However, it can be interpreted in terms of not channelling but 1D motion because the directions
 8 of loop rafts, which is $<111>$, coincides with the direction of 1D motion. Furthermore, we
 9 performed a brief simulation study of channelling behavior in W and found that no significant
 10 difference was observed in the channelling between W{001} and W{011}.

11 Although in this study we attributed the mismatch between the NI hardness profile and
 12 TEM microstructural observation to invisible dislocation loops which are effective to irradiation
 13 hardening, more detailed research on NI hardness profile reflecting the ion-irradiation induced
 14 damage structure distributing with inhomogeneous manner is essential.

15

16 **5 Conclusions**

17 Pure tungsten (W) single crystals of {001} and {011} surface orientations were irradiated
 18 with 6.4 MeV Fe³⁺ ions up to 0.1 and 2 dpa at 573 K. The obtained main results are as follows:

- 19 1) The NI hardness profiles of W single crystals is not significantly influenced by displacement
 20 damage level between 0.1 and 2 dpa, while the profiles show a higher hardening over deeper
 21 indentation depth in W{001} than W{011} irrespective of the displacement level.
- 22 2) Irradiation hardening evaluated by bulk equivalent hardness is already high and shows a
 23 significant orientation dependence at 0.1 dpa. Ion-irradiation hardening of W seems to saturate at
 24 1 dpa.
- 25 3) TEM examinations revealed that the ion-irradiation affected zone was significantly influenced
 26 by the damage level. Although the affected zone depth is similar between W{001} and W{011}
 27 irradiated up to 1 dpa, it becomes so significant at 2 dpa that the affected zone is 1.5 times deeper
 28 in W{001} than in W{011}.

1 4) The double black band structure with a high defect density of ordered networks of dislocation
2 loop rafts was observed in both W{001} and W{011} at 2 dpa as well as 1 dpa, while no such a
3 double band was observed at 0.1 dpa. The formation mechanism of double band structure can be
4 attributed to the mutual annihilation of mobile interstitial dislocation loops and less mobile
5 vacancies and their clusters.
6 5) It is considered that the 1D motion of very fine dislocation loops are invisible by TEM up to 1
7 dpa and becomes large enough to be visible at 2 dpa. Those fine loops are responsible for
8 irradiation hardening irrespective of the loop size.

9

10 **Acknowledgement**

11 The financial support of the first author by the Ministry of Education, Sports, Culture, Science
12 and Technology, MEXT, scholarship of the Japanese Government (1.10.2014 – 30.09.2016) is
13 acknowledged.

14

15

16

1 References

- 2
- 3 [1] Z.X. Zhang, E. Hasenhuettl, K. Yabuuchi and A. Kimura: Nucl. Mater. En. **9** (2016) 539-546.
- 4 [2] D. Armstrong, A. Wilkinson and S.G. Roberts: Physica Scripta **2011 (T145)** (2011) 014076.
- 5 [3] D.E.J. Armstrong, P.D. Edmondson and S.G. Roberts: Applied Physics Letters **102** (25) (2013).
- 6 [4] D.E.J. Armstrong, X. Yi, E.A. Marquis and S.G. Roberts: J. Nucl. Mater. **432** (1-3) (2013) 428-436.
- 7 [5] J.S.K.L. Gibson, S.G. Roberts and D.E.J. Armstrong: Mater Sci Eng A Struct Mater **625** (2015) 380-384.
- 8
- 9 [6] X. Yi, M.L. Jenkins, K. Hattar, P.D. Edmondson, S.G. Roberts: Acta Materialia **92** (2015) 163-177.
- 10
- 11 [7] X. Yi, M.L. Jenkins, M.A. Kirk, Z. Zhou, S.G. Roberts: Acta Materialia **112** (2016) 105-120.
- 12
- 13 [8] S. Kajita, N. Yoshida, N. Ohno, Y. Hirahata, R. Yoshihara: Physica Scripta **89(2)** (2014).
- 14
- 15 [9] F. Liu, H. Ren, S. Peng, K. Zhu: Nucl. Instrum. Methods Phys. Res. B, **333** (2014) 120-123.
- 16
- 17 [10] G. Ran, S. Wu, X. Liu, J. Wu, N. Li, X. Zu and L. Wang: Nucl. Instrum. Methods Phys. Res. B **289** (2012) 39-42.
- 18
- 19 [11] Y. Yuan, H. Greuner, B. Böswirth, C. Linsmeier, G.N. Luo, B.Q. Fu, H.Y Xu, Z.J.Shen and W. Liu: J. Nucl. Mater. **437** (2013) 297-302.
- 20
- 21 [12] J. Grzonka, L. Ciupinski, J. Smalc-Koziorowska, O.V. Ogorodnikova, M. Mayer, K.J. Kurzydlowski: Nucl. Instrum. Methods Phys. Res. B **340** (2014) 27-33.
- 22
- 23 [13] E. Hasenhuettl, Z.X. Zhang, K. Yabuuchi, P. Song and A. Kimura: Nucl. Instrum. Methods Phys. Res. B, B **397** (2017) 11-14 <http://dx.doi.org/10.1016/j.nimb.2017.02.030>.
- 24
- 25 [14] W. D. Nix and H. Gao: J. Mechan. Phys. Solids **46** (1998) 411-425.
- 26
- 27 [15] R. Kasada, Y. Takayama, K. Yabuuchi and A. Kimura: Fus. Eng. Des. **86** (2011) 2658-2661.
- 28
- 29 [16] J. F. Ziegler and J. P. Biersack, SRIM – The Stopping Range of Ions in Matter, James Ziegler, 2009 <http://www.srim.org/>.
- [17] R. E. Stoller, M. B. Toloczko, G. S. Was, A. G. Certain, S. Dwaraknath and F. A. Garner: Nucl. Instrum. Methods Phys. Res. B **310** (2013) 75-80.

- 1 [18] ASTM Standard Practice for Neutron Radiation Damage Simulation by Charged-Particle
2 Irradiation **E521-96** (2009).
- 3 [19] W. C. Oliver and G. M. Pharr: J. Mater. Res. **19** (2004) 3-20.
- 4 [20] E. Hasenhuettl, R. Kasada, Z. X. Zhang, K. Yabuuchi, Y.-J. Huang and A. Kimura: Mater.
5 Trans. **58** (2017) 749-756.
- 6 [21] W. C. Oliver and G. M. Pharr: J. Mater. Res. **7** (1992) 1564-1583.
- 7 [22] I. Manika and J. Maniks: J. Phys. D **41** (2008) p. 074010.
- 8 [23] C. K. Dolph, D. J. da Silva, M. J. Swenson and J. P. Wharry: J. Nucl. Mater. **481** (2016) 33-
9 45.
- 10 [24] P. Dayal, D. Bhattacharyya, W. M. Mook, E. G. Fu, Y.-Q. Wang, D. G. Carr, O. Anderoglu,
11 N. A. Mara, A. Misra, R. P. Harrison and L. Edwards: J. Nucl. Mater. **438** (2013) 108-115.
- 12 [25] P. [22] Hosemann, D. Kiener, Y. Wang and S. A. Maloy: J. Nucl. Mater. **425** (2012) 136-
13 139.
- 14

1 **Tables**

		W{001}			W{011}			
		0.1 dpa	1 dpa	2 dpa	unirr.	0.1 dpa	1 dpa	2 dpa
$H_{bulkequiv.}$ [GPa]	4.2	8.0	8.7	9.3	4.5	6.6	8.8	9.2
ΔH [GPa]		3.8	4.5	5.1		2.1	4.3	4.7
$h_{crit.no1}$ [nm]		480	480	630		360	380	480
$h_{crit.no2}$ [nm]		830	1000	1300		no	no	no

2

3 Table 1: Summary of bulk equivalent hardness, irradiation hardening and h_{crit} (for a
4 representative indentation marked in Fig. 2).

5

6

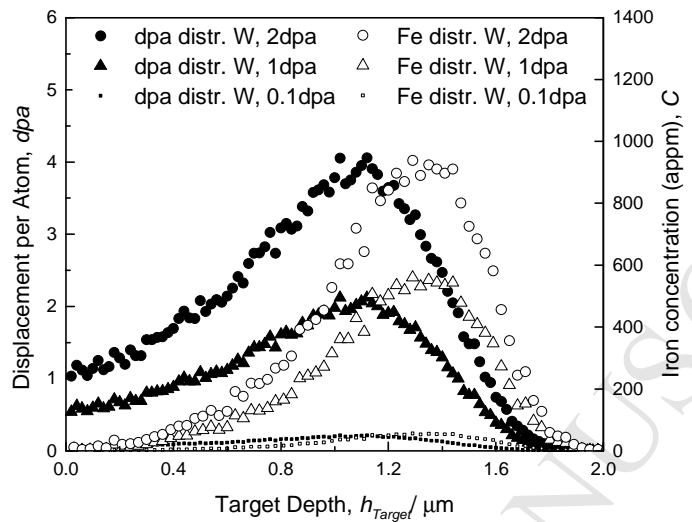
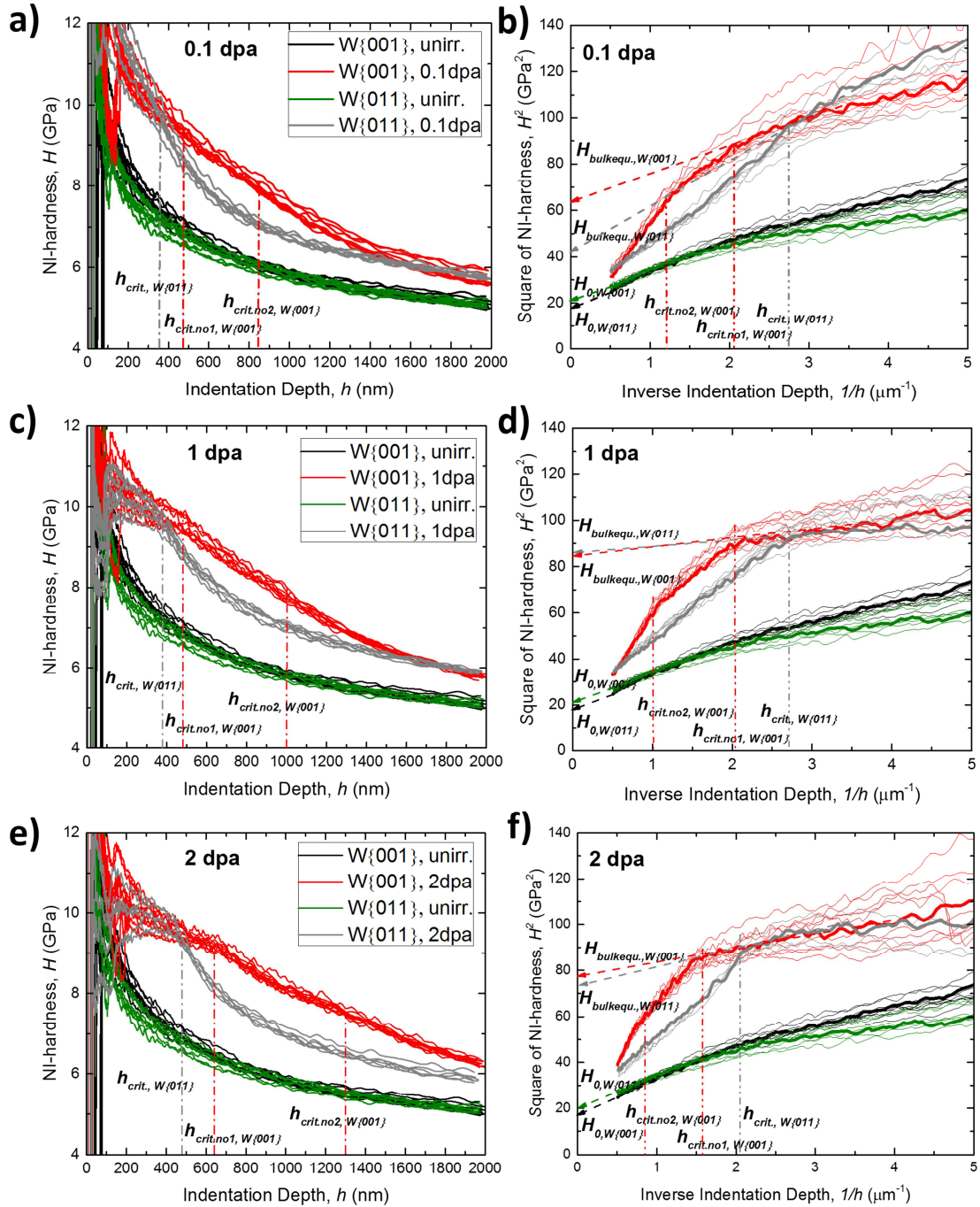
Figures

Fig. 1: Damage and iron distribution in W single crystal of nominal 0.1, 1 [13] and 2 dpa.

1



2

3 Fig. 2: a), c) and e) show the H - h profile and b), d) and f) show H^2 - $1/h$ profile of unirradiated and
4 irradiated W single crystals to 0.1 dpa (a) and b)), 1 dpa (c) and d)) [13] and 2 dpa (e) and f)).

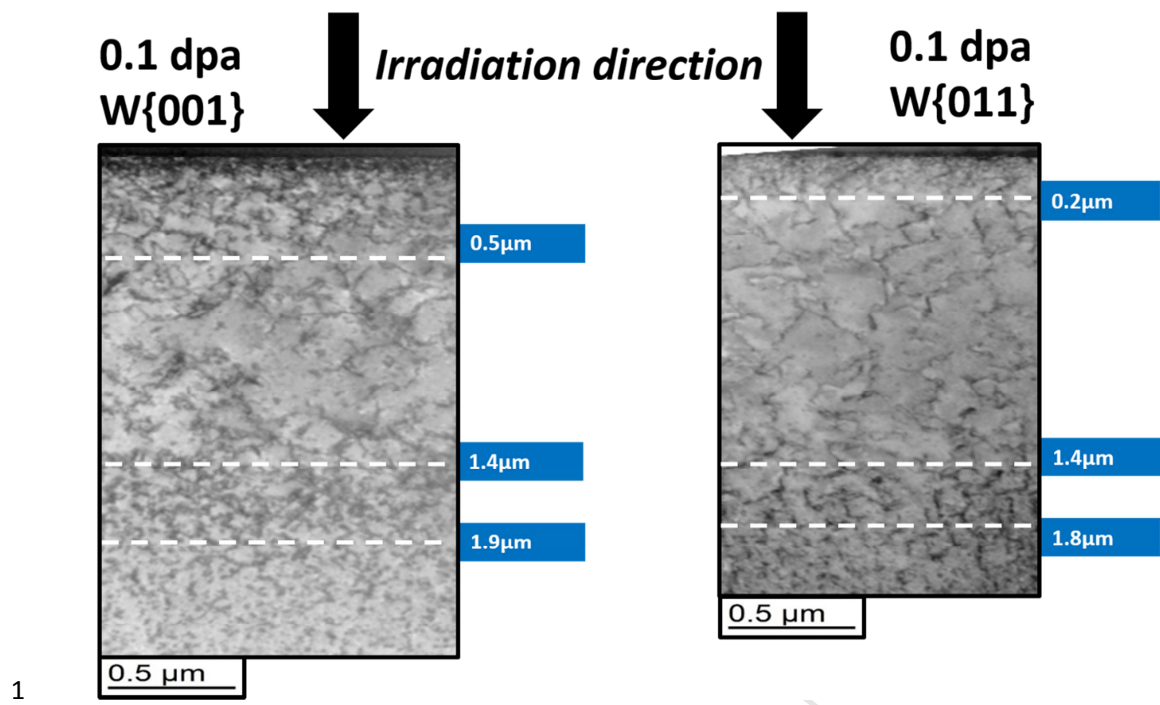


Fig. 3: Microstructural overview of 0.1 dpa $W\{001\}$ and 0.1 dpa $W\{011\}$. The depth of ion-irradiation affected zone is very similar in both orientations.

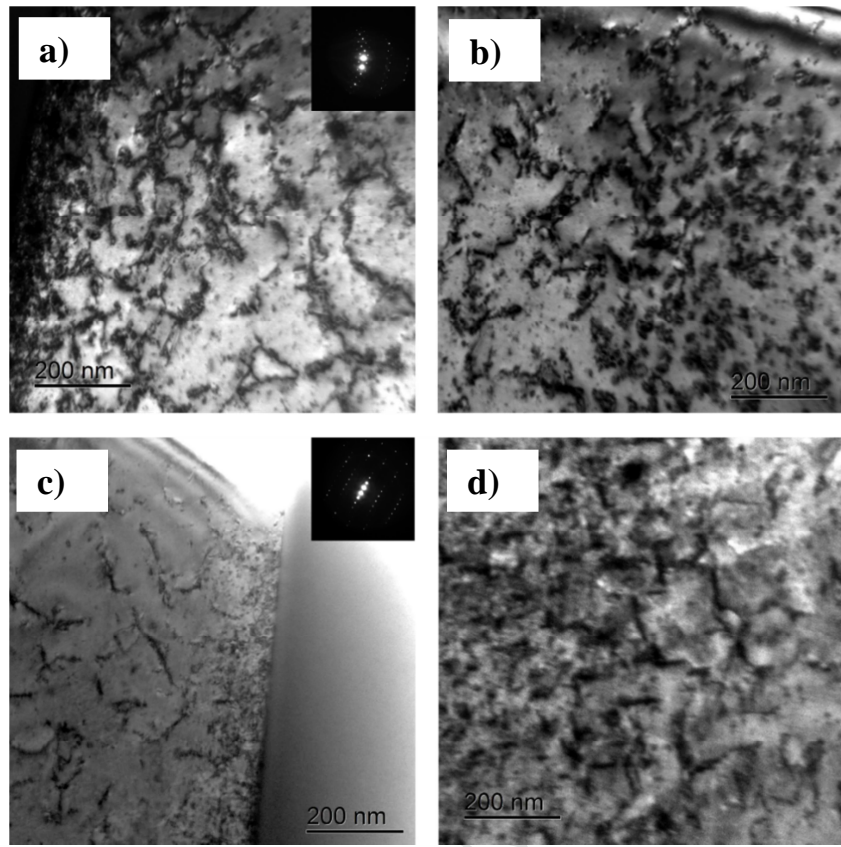
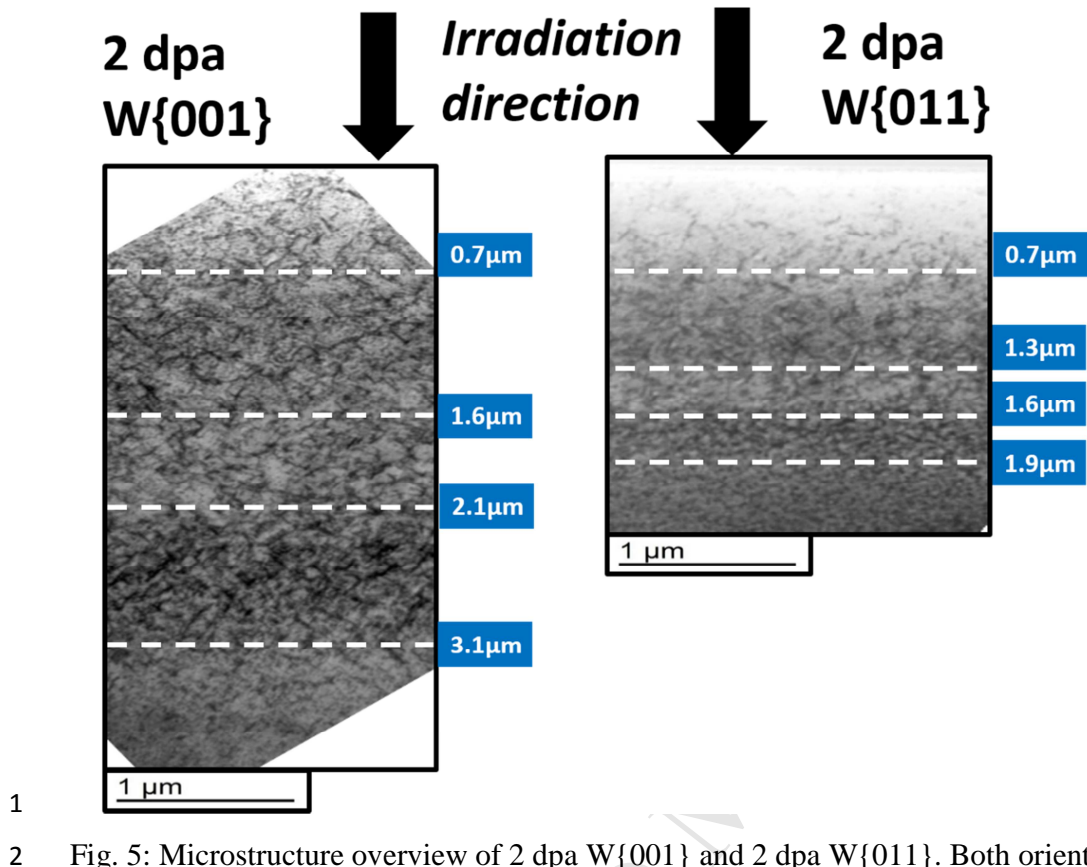


Fig. 4: Microstructural overview of 0.1 dpa W{001}: a) Irradiation surface detail; b) black band detail. Microstructural overview of 0.1 dpa W{011}: c) Irradiation surface detail; d) black band detail.



1 Fig. 5: Microstructure overview of 2 dpa W{001} and 2 dpa W{011}. Both orientations show
2 two high defect density bands, mostly consisting of dislocation loop rafts. The position of ion-
3 irradiation affected zone is much deeper in W{001}.
4
5

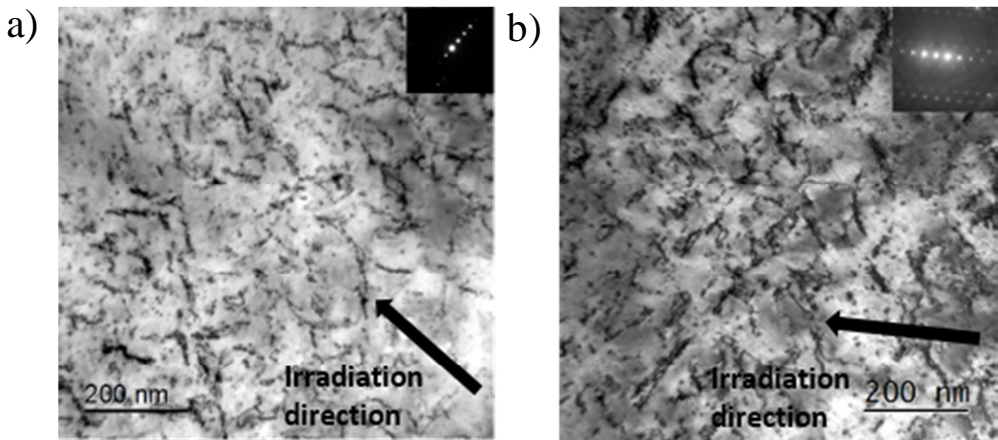


Fig. 6: Microstructural detail of the deeper black band consisting of an ordered network of loop rafts in the direction parallel to $<111>$ in a) 2 dpa W{001} and b) 2 dpa W{001}.

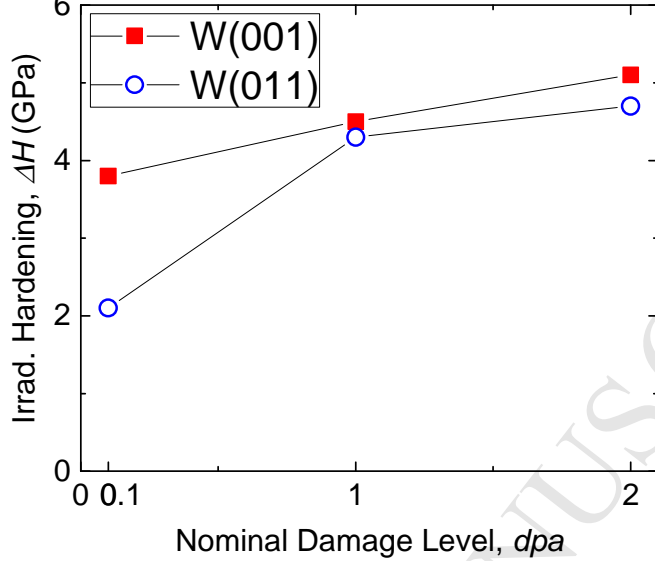
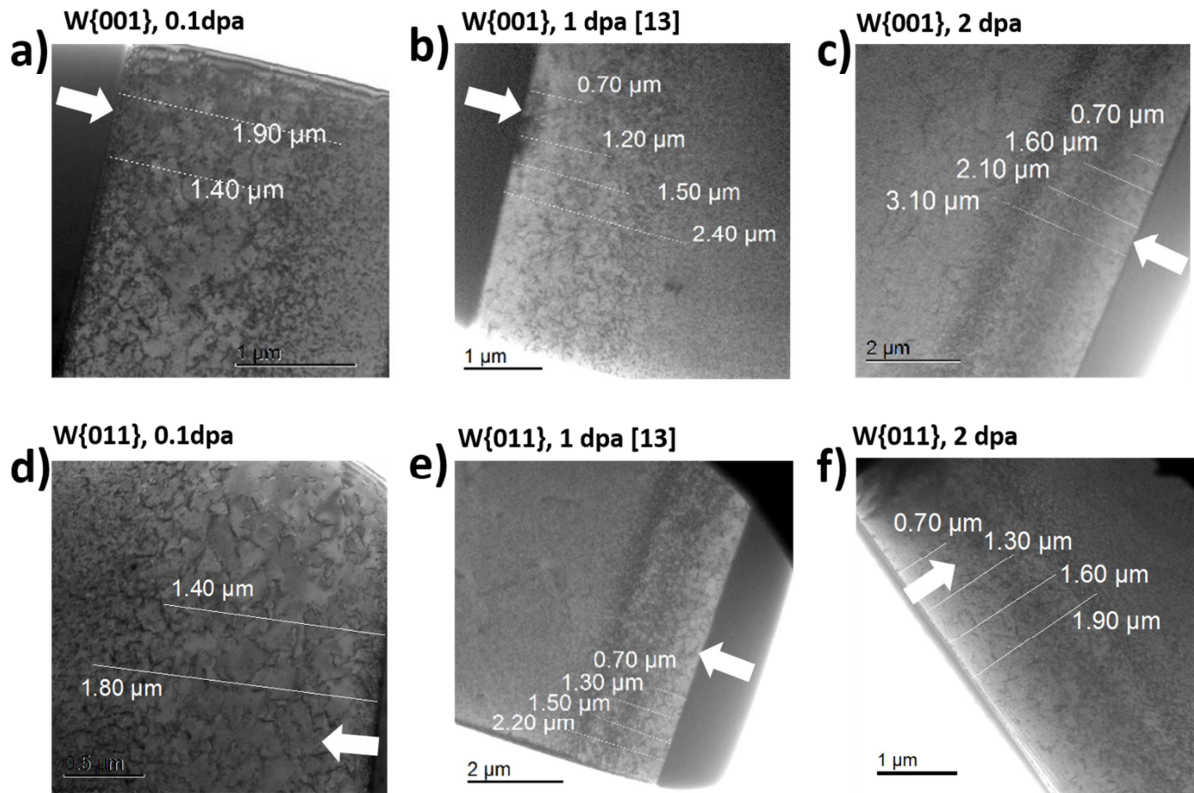


Fig. 7: Irradiation hardening as a function of nominal damage level (for a representative indentation marked in Fig. 2).

1



2

3 Fig. 8: Summary of ion-irradiation damaged zone as a function of crystal orientation and damage
4 level: a) 0.1 dpa W{001}, b) 1 dpa W{001}, c) 2 dpa W{001}, d) 0.1 dpa W{011}, e) 1 dpa
5 W{011} and f) 2 dpa W{011}.

6